Available online at www.sciencedirect.com
ScienceDirect
Polymer 48 (2007) 4213–4225
polymer
www.elsevier.com/locate/polymer

Poly(L-lactide)/nano-structured carbon composites: Conductivity, thermal properties, crystallization, and biodegradation

Hideto Tsuji [a,*], Yoshio Kawashima [a], Hirofumi Takikawa [b], Saburo Tanaka [a]

[a] Department of Ecological Engineering, Faculty of Engineering, Toyohashi University of Technology, Tempaku-cho, Toyohashi, Aichi 441-8580, Japan
[b] Department of Electrical and Electronic Engineering, Faculty of Engineering, Toyohashi University of Technology, Tempaku-cho, Toyohashi, Aichi 441-8580, Japan

Received 23 January 2007; received in revised form 11 May 2007; accepted 11 May 2007
Available online 24 May 2007

Abstract

The effects of nano-structured carbon fillers [fullerene C_{60}, single wall carbon nanotube (SWCNT), carbon nanohorn (CNH), carbon nanoballoon (CNB), and ketjenblack (KB)] and conventional carbon fillers [conductive grade and graphitized carbon black (CB)] on conductivity (resistance), thermal properties, crystallization, and proteinase K-catalyzed enzymatic degradation of poly(L-lactide) [i.e., poly(L-lactic acid) (PLLA)] films were investigated. Even at low filler concentrations such as 1 wt%, the addition of SWCNT effectively decreased the resistivity of PLLA film compared with that of conventional CB, and PLLA–SWCNT film with filler concentration of 10 wt% attained the resistivity lower than 100 Ω cm. The crystallization of PLLA further decreased the resistivity of films. The addition of carbon fillers, except for C_{60} and CNB at 5 wt%, lowered the glass transition temperature, whereas the addition of carbon fillers, excluding C_{60}, elevated softening temperatures, if an appropriate filler concentration was selected. On heating from room temperature, cold crystallization temperature was determined mainly by the molecular weight of PLLA, whereas on cooling from the melt, the carbon fillers, excluding KB, elevated the cold crystallization temperature, reflecting the effectiveness of most of the carbon fillers as nucleating agents. Despite the nucleating effects, the addition of carbon fillers decreased the enthalpy of cold crystallization of PLLA on both heating and cooling. The addition of CNH, CNB, and CB elevated the starting temperature of thermal degradation of PLLA, whereas the addition of SWCNT reduced the thermal stability. Furthermore, the addition of C_{60} and SWCNT enhanced the enzymatic degradation of PLLA, whereas the addition of KB and CNB disturbed the enzymatic degradation of PLLA. The reasons for the effects of carbon fillers on the physical properties, crystallization, and enzymatic degradation of PLLA films are discussed.

Keywords: Poly(lactic acid); Polylactide; Nano-structured carbons

1. Introduction

Biomass-derived poly(L-lactide), i.e., poly(L-lactic acid) (PLLA) has been intensively explored because it is biodegradable, compostable, producible from renewable resources, and nontoxic to the human body and the environment. The improvement of physical properties of PLLA, such as mechanical, thermal, and electrical ones, is a matter of concern, especially when used in industrial and commodity applications [1–12]. For improvement of these properties, the addition of various types of fillers is commercially advantageous, because the physical properties are readily manipulated by the type and concentration of fillers. Talc and montmorillonite are representative cost-effective fillers for PLLA to improve crystallinity, thermal stability, and mechanical properties [13–19].

In our previous study, we investigated the nucleating effects of fullerene C_{60} and poly(D-lactide), i.e., poly(D-lactic acid) (PDLA) (or the stereocomplex crystallites formed upon addition of PDLA to PLLA) on the crystallization behavior of PLLA [19,20]. It was found that the acceleration effects of fillers on the overall PLLA crystallization during cooling from the melt decreased in the following order: PDLA >

* Corresponding author.
E-mail address: tsuji@eco.tut.ac.jp (H. Tsuji).

0032-3861/$ - see front matter © 2007 Elsevier Ltd. All rights reserved.
doi:10.1016/j.polymer.2007.05.040

talc > C_{60} > montmorillonite > polysaccharides, and the acceleration effects of PDLA widely varied depending on its concentration. The positive effect of PDLA on the overall crystallization was observed when the concentration of PDLA was higher than 3 wt%. However, as far as we are aware, the effects of carbon-nanostructured fillers on the physical properties, crystallization, and biodegradation of PLLA have not been reported so far, excluding those of fullerene C_{60}.

The objective of the present study was to investigate the effects of addition of the various carbon-nanostructured fillers on the physical properties, crystallization, and biodegradation of PLLA. For this purpose, we have prepared melt-quenched PLLA films with fullerene C_{60}, single wall carbon nanotube (SWCNT), carbon nanohorn (CNH), carbon nanoballoon (CNB), and ketjenblack (KB), together with those with carbon black (CB). Their conductivity (resistivity), thermal properties, crystallization behavior, and biodegradation behavior were studied by four-point probe array, thermomechanical analysis (TMA), differential scanning calorimetry (DSC), thermogravimetry (TG), gravimetry, and scanning electron microscopy (SEM).

2. Experimental part

2.1. Materials

PLLA [number-average molecular weight (M_n) = 9.5 × 10^4 g mol^{-1}, weight-average molecular weight (M_w)/M_n = 1.9, specific optical rotation ($[\alpha]_{589}^{25}$) = −141 deg dm^{-1} g^{-1} cm^3] was kindly supplied by Unitika Ltd. (Osaka, Japan) and was purified by precipitation using methylene chloride and methanol as solvent and nonsolvent, respectively. The purified polymer was dried in vacuo for at least 7 days. C_{60} (>99.5%, particle size of 1 nm), KB (EC600JD, primary particle size of 34 nm), and conductive grade CB (TOKABLACK™#5500, particle size of 25 nm, abbreviated as CB5500) and graphitized CB (TOKABLACK™#3855, particle size of 25 nm, abbreviated as CB3855) were supplied from Tokyo Chemical Industry Co. Ltd. (Tokyo, Japan), Ketjen Black International Company Ltd. (Tokyo, Japan), and Tokai Carbon Co. Ltd. (Tokyo, Japan), respectively. SWCNT was prepared by a conventional arc discharge method, where the graphite rod containing Ni (4.2 mol%)/Y (1 mol%) catalyst (KM42NI10Y, 6 mm in diameter, Toyo Tanso Co. Ltd., Osaka, Japan) was used as evaporating electrode (anode). Cathode was pure graphite (G348, Tokai Carbon Co. Ltd.). The ambient gas was helium and the pressure was approximately 80 kPa. SWCNT (average diameter = 1.5 nm, average length = 3 μm) used in the present study was not purified so that the metal catalyst and amorphous carbon coexisted. The products included 30–50 wt% of SWCNT. CNH was prepared in the same arc discharge system which was used for preparing SWCNT [21,22]. However, the condition was different. The anode and cathode were pure graphite (G348). The ambient gas was nitrogen and the pressure was approximately 90 kPa. The products included more than 35% of Dahlia-type CNH. Most of the rest was non-Dahlia-type CNH. CNB was prepared from the non-Dahlia-type CNH by high temperature treatment (approximately 2400 °C) under inert gas [21,22]. Non-Dahlia-type CNH was prepared at 80 kPa of nitrogen by arc discharge method.

The PLLA films with fillers C_{60}, SWCNT, CNH, CNB, and KB, together with those with CB were prepared by a solution-casting method using dichloromethane as a solvent at 25 °C for approximately 1 day. The solutions for casting were prepared by dissolving 3 g of PLLA and a filler in 10 mL of dichloromethane. The obtained films were dried in vacuo for at least 7 days, and then were further melt-blended (ca. 2 g for each sample) with a kneading extruder (Type 1172, Imoto Machinery Co. Ltd., Kyoto, Japan) at 200 °C and 20 rpm for 5 min. After the melt-blending process, the blends were extruded and then compressed between two polyimide sheets to a thickness of 200 μm using Teflon spacers with the same thickness.

The concentration of each of the fillers was fixed at 5 and 10 wt% for the PLLA films, unless otherwise specified. All the melt-blend films were amorphous. This was evidenced by the same absolute values of the enthalpies of crystallization and melting. Some of the melt-blend films were further crystallized by the following procedure. Each of the melt-blend films was sealed under a reduced pressure, re-melted at 200 °C for 5 min and crystallized at 140 °C for 24 h, and then quenched at 0 °C. The PLLA films with fillers are abbreviated as PLLA–a filler code (''number'' here indicates the concentration of a filler or ''C'' here means that the specimen was crystallized by aforementioned procedure), e.g., PLLA–CNH for the PLLA film with CNH, PLLA–SWCNT(10) for the PLLA film with 10 wt% of SWCNT, and PLLA–CB3855(C) for the crystallized PLLA film with CB3855.

2.2. Enzymatic degradation

The enzymatic degradation of the films with 10 wt% of fillers was performed according to the procedure reported by Reeve et al. [23]. Namely, each of the films was placed in a vial filled with 5 mL of Tris–HCl buffer solution (pH 8.6) containing 0.2 mg mL^{-1} of proteinase K and 0.2 mg mL^{-1} of sodium azide. The enzymatic degradation of the films was carried out at 37 °C in a rotary shaker for a period of up to 3 h. The pH of the solution remained in the range between 8.6 and 8.0 for 3 h, where the enzyme activity was reported to be practically constant [23]. The degraded films were rinsed thoroughly with the distilled water at 4 °C to stop further degradation and then dried under a reduced pressure for at least 2 weeks for weight loss measurements.

2.3. Measurements and observation

The weight- and number-average molecular weights (M_w and M_n, respectively) of polymers were evaluated in chloroform at 40 °C using a Tosoh (Tokyo, Japan) GPC system with two TSK gel columns (GMH_{xL}) using polystyrene standards. The $[\alpha]_{589}^{25}$ was measured in chloroform at a concentration of

1 g dL^{-1} and 25 °C using a JASCO (Tokyo, Japan) DIP-140 polarimeter at a wave length of 589 nm.

The resistivity (conductivity) of the films was measured according to the method JIS K7194 (testing method for resistivity of conductive plastics with a four-point probe array). Namely, four-point probes (spring probe VP-3-1 and socket VS-3-1, Mac-Eight Co. Ltd., Kanagawa, Japan) were placed in-line, and then the potential difference between the probes B and C (V) was measured with a 34401A Digital Multimeter (Agilent Technologies Japan, Ltd., Tokyo, Japan) when the electric current (I) was passed from probe A to probe D (see Fig. 1). The resistivity (ρ) was calculated from an obtained resistance value ($R = V/I$) using the following equation:

$$\rho(\Omega\,\mathrm{cm}) = F \times d \times R \tag{1}$$

where F and d are correction factor (4.235) and film thickness (cm), respectively. The experimental ρ values represent averages of measurements at five different positions of the films and the absolute value of the difference between the each experimental value and the average value was lower than 5% of the average value.

The softening temperature of PLLA films with different fillers was measured with a penetration mode at an applied load of 0.98 N using a Shimadzu (Kyoto, Japan) TMA-60 under a nitrogen gas flow at a rate of 50 mL min^{-1}. The specimens (thickness of 200 μm) were heated from room temperature to 140 °C at a rate of 7 °C min^{-1}. The glass transition and crystallization behavior of PLLA films (sample weight ca. 3 mg) with different fillers were monitored by a Shimadzu DSC-50 differential scanning calorimeter under a nitrogen gas flow at a rate of 50 mL min^{-1}. The specimens were heated at a rate of 10 °C min^{-1} from room temperature to 200 °C (Process I), held at the same temperature for 5 min, and then cooled at a rate of −3 °C min^{-1} to room temperature (Process II). The glass transition, cold crystallization, and melting temperatures (T_g, T_{cc}, and T_m, respectively) and the enthalpies of cold crystallization (ΔH_{cc}) and melting (ΔH_m) were calibrated using benzophenone, indium, and tin as standards. Normalized ($-\Delta H_{cc}$) was calculated from non-normalized ($-\Delta H_{cc}$) according to the following equation:

$$\text{Normalized}(-\Delta H_{cc})\left(\mathrm{J\,g^{-1}}\right) = \text{non-normalized}(-\Delta H_{cc})\left(\mathrm{J\,g^{-1}}\right)/[1 - W(A)/100] \tag{2}$$

where $W(A)$ is weight percentage of a filler in the film. The thermal degradation behavior of PLLA films with different fillers was traced by TG using a Shimadzu DTG-50. The specimens (sample weight ca. 3 mg) were heated from room temperature to 420 °C at a rate of 10 °C min^{-1} under a nitrogen gas flow of 50 mL min^{-1}. The surface morphology of the enzymatically degraded films was studied with a Hitachi (Tokyo, Japan) SEM (S-2300). The specimens for SEM observation were coated with carbon to a thickness of about 10 nm. Some of the nano-structured carbon materials were observed with a JEOL (Tokyo, Japan) JEM2010 transmission electron microscope (TEM). Fig. 2 shows the structural models and typical TEM images of SWCNT, CNH, and CNB.

The weight loss per unit surface area of the enzymatically degraded films [W_{loss} (μg mm^{-2})] was calculated using the weights of dried films before and after enzymatic degradation (W_{before} and W_{after}), respectively, and their surface area before enzymatic degradation (S_{before}):

$$W_{loss}\left(\mu\mathrm{g\,mm^{-2}}\right) = \left(W_{before} - W_{after}\right)/S_{before} \tag{3}$$

The experimental weight loss values for enzymatic degradation represent averages of measurements from the three replicate specimens.

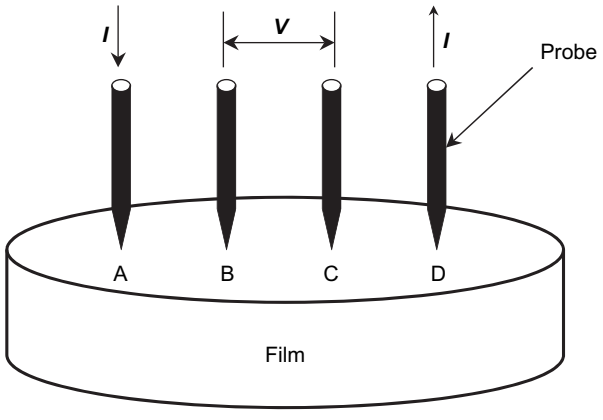

Fig. 1. The schematic representation of testing method for resistivity of conductive plastics with a four-point probe array.

3. Results and discussion

3.1. Conductivity

The ρ values of PLLA films decreased with increasing filler concentration, as shown in Fig. 3. For the polymer/CB composites, it is reported that the material conductivity is affected by the shape, size, dispersion state, and conductivity of CB, and other factors [24–26]. Among the carbon fillers, SWCNT and CB3855 (graphitized carbon black) showed the remarkable effects on the ρ of PLLA films. That is, PLLA–SWCNT and PLLA–CB3855 showed the lowest and second lowest ρ values or the highest and second highest conductivity values among the PLLA films. Therefore, we have carried out the detailed investigation on the effects of concentration of SWCNT and CB3855 on the ρ values of PLLA films (Fig. 4). The ρ values of PLLA–SWCNT and PLLA–CB3855 decreased from 1.6×10^5 Ω cm at a filler concentration of 0 wt% to the values lower than 1×10^2 Ω cm at a filler concentration of 10 wt%. The ρ values were lower for PLLA–SWCNT films than for PLLA–CB3855 films, when compared at the same filler concentrations. The needle-like (fiber-like) structure of SWCNT should have caused its effective contact with each other compared with that of more spherical other fillers, and thereby have given the lowest ρ values. It is interesting to note that even the addition of 1 wt% of SWCNT induced a dramatic decrease in ρ from 1.6×10^5 to 3.8×10^3 Ω cm. Such

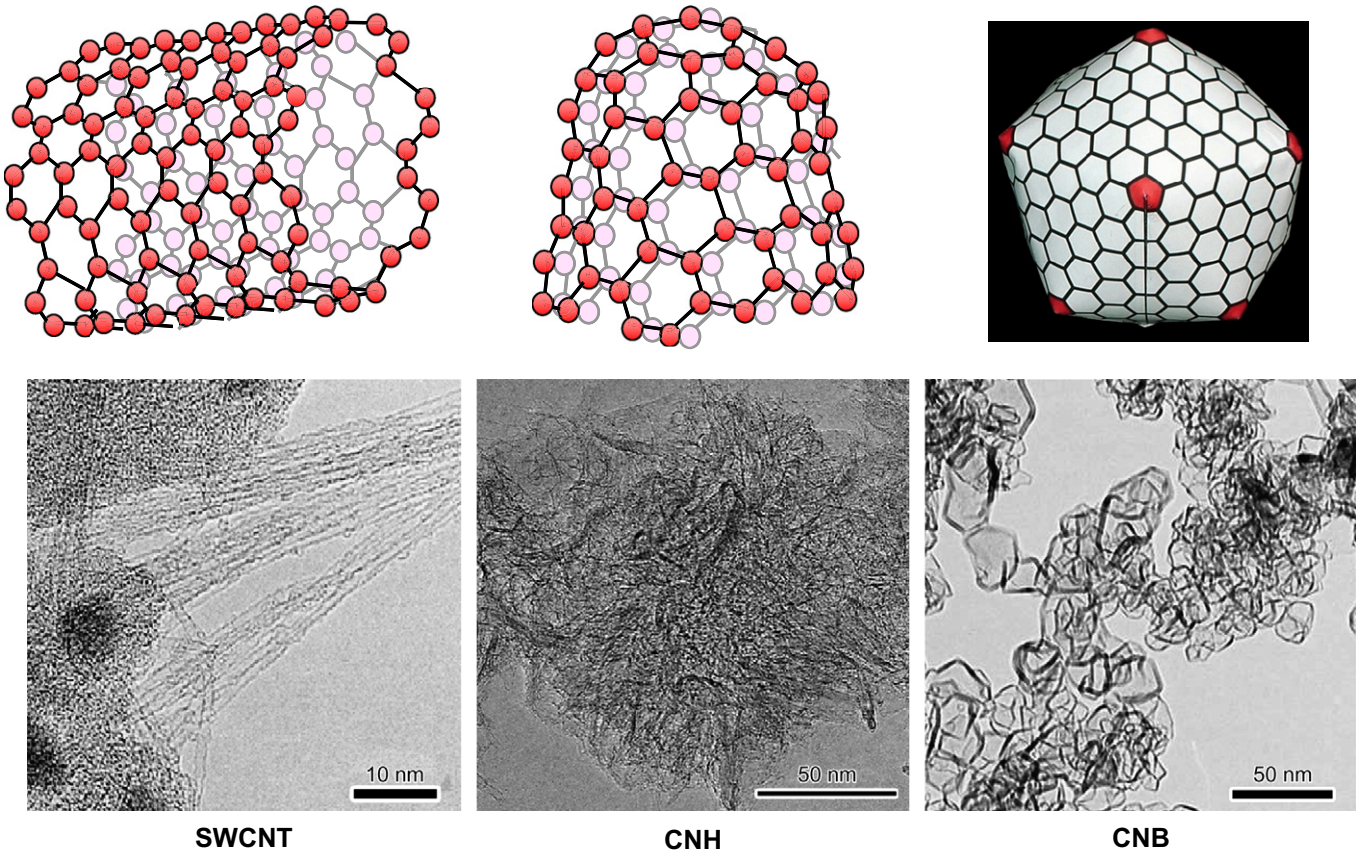

Fig. 2. The structural models and typical TEM images of SWCNT, CNH, and CNB.

a remarkable effect was not observed for conventional carbon black (CB3855). It is reported that when a particulate conducting filler is added to a nonconducting matrix, a sharp transition from nonconductor to conductor takes place at a critical concentration at around 7 wt% [24]. The effectiveness of SWCNT on the conductivity of PLLA films even at 1 wt% indicates that the critical concentration for SWCNT should be lower than 1 wt%. Such a low critical concentration for SWCNT is also attributable to its needle-like structure, which obliges SWCNT to effectively contact with each other.

In an amorphous state the carbon fillers are homogeneously dispersed. However, such a state is not favorable for increasing conductivity of the PLLA films. During crystallization process, the carbon filler as an impurity will be excluded from the crystalline regions and condensed in the amorphous regions. As a result, the conductive fillers are expected to be effectively connected with each other in amorphous regions, and thereby increased the conductivity compared with that in a completely amorphous state. To confirm this assumption, each of the PLLA–SWCNT and PLLA–CB3855 films was sealed under a reduced pressure, melted at 200 °C for 5 min, crystallized at 140 °C for 24 h, quenched at 0 °C, and then their ρ values were estimated. The obtained ρ values of the films are included in Fig. 4. As expected, the ρ values of crystallized PLLA–SWCNT(C) and PLLA–CB3855(C) films were lower than those of the amorphous PLLA–SWCNT and PLLA–CB3855 films, respectively, when compared at the same filler concentrations. The PLLA–SWCNT(C) films showed the lowest ρ (highest conductivity) at a filler concentration of 10 wt% (26 Ω cm), which is comparable with that reported for a hydrocarbon wax ($C_{36}H_{74}$) containing CB (7.6 vol%) [24]. Bueche showed that the ρ of a hydrocarbon wax ($C_{36}H_{74}$) containing CB suddenly increased at the

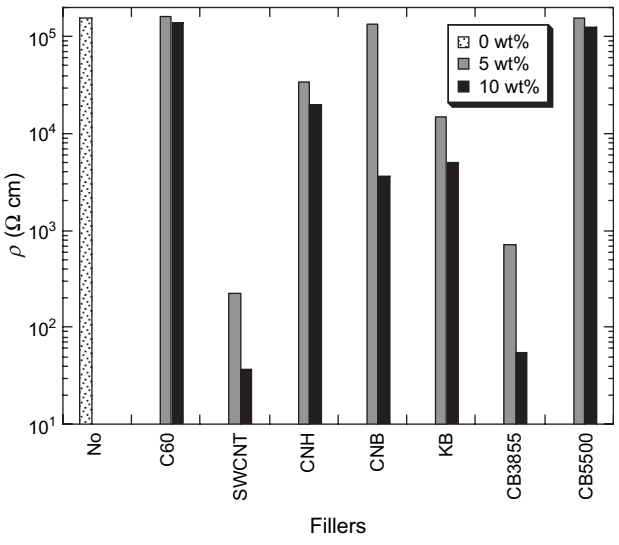

Fig. 3. Resistivity (ρ) of PLLA films with different carbon fillers at 5 and 10 wt%.

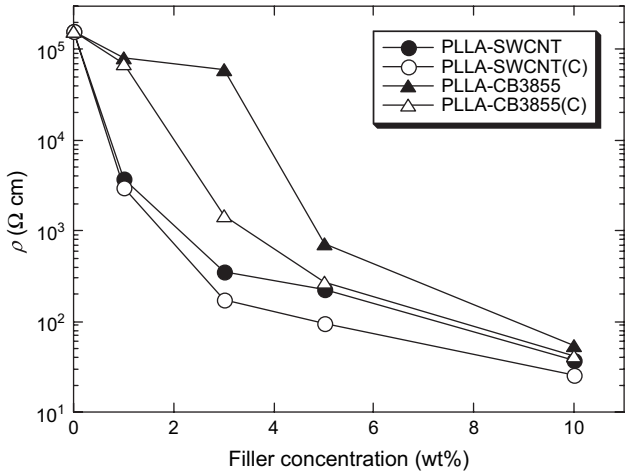

Fig. 4. Resistivity (ρ) of PLLA–SWCNT and PLLA–CB3855 films at different carbon filler concentrations.

temperature above the melting temperature of hydrocarbon wax [24]. Recently, Lee et al. and Chen et al., respectively, reported the same trend for the blends of poly(ε-caprolactone) and poly(vinylbutyral) containing CB [26] and for the methyl methacrylate copolymer and ultrahigh molecular weight of polyethylene composites filled with multiwall carbon nanotubes [27]. Compared with the conventional CB, the effectiveness of SWCNT for increasing conductivity of PLLA films was higher especially at a low concentration. This strongly suggests that SWCNT can be a promising filler to enhance the conductivity of PLLA-based materials.

3.2. Softening behavior

The T_g values, starting and ending softening temperatures [T_{soft}(S) and T_{soft}(E), respectively] of PLLA films with different carbon fillers at 5 and 10 wt% during heating from room temperature (Process I) were obtained from DSC and TMA curves, and are shown in Fig. 5 and Table 1. The procedures for estimating T_{soft}(S) and T_{soft}(E) are shown in Fig. 6. That is, T_{soft}(S) and T_{soft}(E) are the intersection temperatures of the base lines for lower and higher temperature ranges and the tangent line for the curve. As seen from Fig. 5, the T_g values of PLLA films with the fillers, except for PLLA–C_{60}(5) and PLLA–CNB(5) films, were lower than that of pure PLLA film, revealing that the chain mobility of PLLA was enhanced by the presence of most of the carbon fillers. Despite this fact, the carbon fillers, except for C_{60}, were effective to elevate both T_{soft}(S) and T_{soft}(E) values, if an appropriate concentration was selected. It seems that the molecular (particle) size of C_{60} was too small to support the external force on heating.

As shown in Table 1, the molecular weight values of PLLA films after thermal molding depend on the types of carbon fillers. The molecular weight of PLLA should have affected the T_g, T_{soft}(S), and T_{soft}(E) values of the films. For this reason, the T_g, T_{soft}(S), and T_{soft}(E) values of the PLLA films

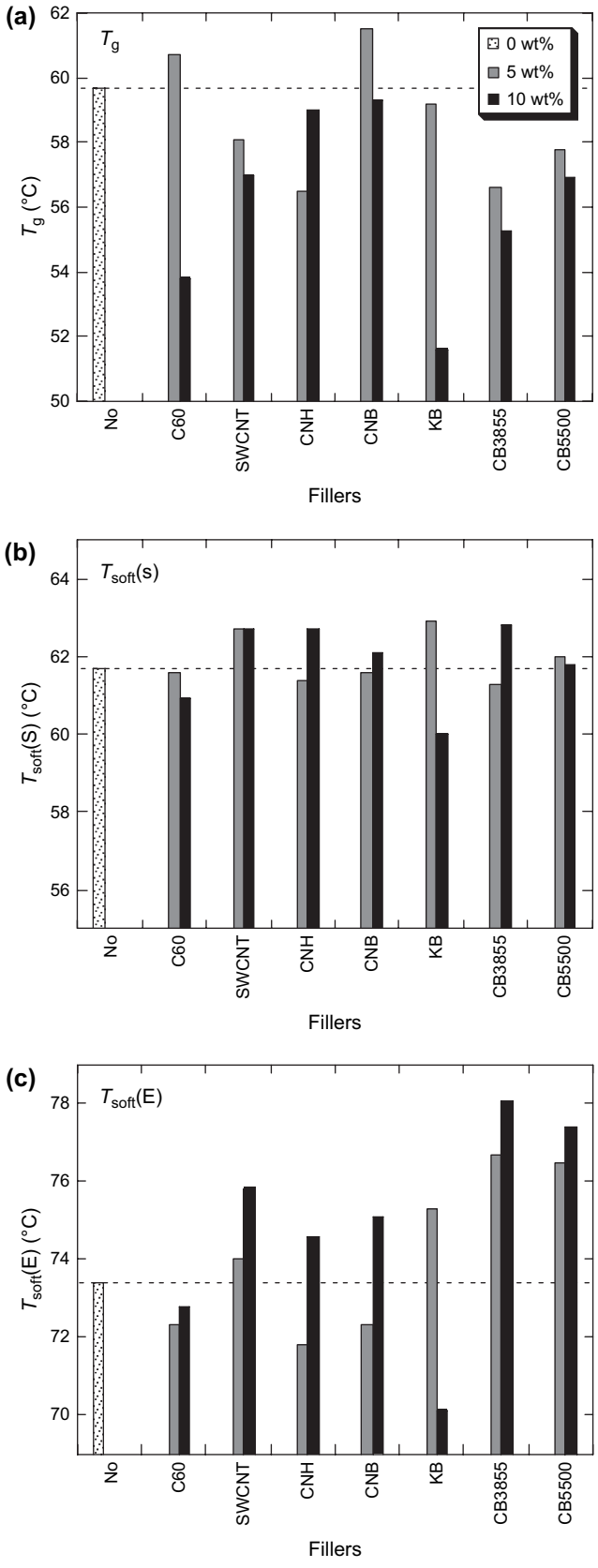

Fig. 5. Glass transition temperature (T_g) (a), starting and ending softening temperatures [T_{soft}(S) (b) and T_{soft}(E) (c), respectively] of PLLA films with different carbon fillers (5 and 10 wt%) during heating from room temperature (Process I). Horizontal broken lines show the values for pure PLLA film.

Table 1
The glass transition temperature and the starting and ending temperatures of softening and thermal degradation of pure PLLA film and PLLA films with different fillers

Filler	Content (wt%)	$M_w/10^4$ (g mol^{-1})	M_w/M_n	T_g[a] (°C)	T_{soft}(S)[b] (°C)	T_{soft}(E)[b] (°C)	T_{td}(S)[c] (°C)	T_{td}(E)[c] (°C)
No	0	6.1	1.8	59.7	61.7	73.4	295.3	363.7
C_{60}	5			60.7	61.6	72.3	312.5	370.2
	10	3.2	1.7	53.8	60.9	72.8	290.5	341.3
SWCNT	5			58.1	62.7	74.0	279.2	344.6
	10	3.3	2.5	57.0	62.7	75.8	266.4	323.1
CNH	5			56.5	61.4	71.8	314.7	364.2
	10	6.3	1.8	59.0	62.7	74.6	328.4	366.7
CNB	5			61.5	61.6	72.3	337.6	372.9
	10	5.0	1.9	59.3	62.1	75.1	317.0	371.1
KB	5			59.2	62.9	75.3	333.3	372.9
	10	3.2	2.2	51.6	60.0	70.1	290.9	362.5
CB3855	5			56.6	61.3	76.7	308.2	362.8
	10	11.9	1.7	55.3	62.8	78.1	335.2	373.3
CB5500	5			57.8	62.0	76.5	341.8	375.0
	10	16.6	2.1	56.9	61.8	77.4	338.2	373.1

[a] Glass transition temperature.
[b] T_{soft}(S) and T_{soft}(E) are the starting and ending temperatures of softening, respectively.
[c] T_{td}(S) and T_{td}(E) are the starting and ending temperatures of thermal degradation, respectively.

containing 10 wt% of fillers are plotted in Fig. 7 as a function of M_w. All T_g values of PLLA films with carbon fillers were significantly lower than that of pure PLLA film, irrespective of the M_w. This confirms that the chain mobility of PLLA was enhanced by the presence of carbon fillers, irrespective of the M_w. On the other hand, the T_{soft}(S) values of the PLLA films were almost constant for the M_w exceeding 5×10^4 g mol^{-1}, whereas the T_{soft}(E) values increased with an increase in M_w. The T_{soft}(S) and T_{soft}(E) values of the PLLA films, except for PLLA–C_{60} and PLLA–KB films, were higher than those of the pure PLLA film, irrespective of M_w of PLLA. This reveals that most of the carbon fillers are effective to elevate the dimensional stability of PLLA films on heating.

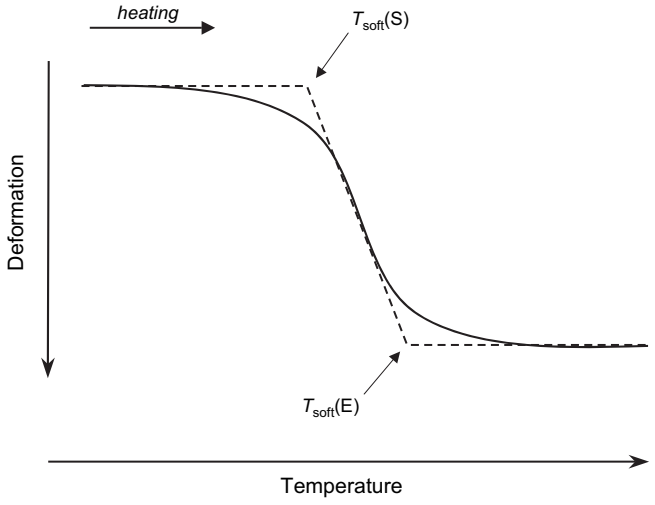

Fig. 6. Procedures for estimating the starting and ending softening temperatures [T_{soft}(S) and T_{soft}(E), respectively].

3.3. Crystallization

The cold crystallization temperatures, T_{cc}(S), T_{cc}(P), and T_{cc}(E) of PLLA films with different carbon fillers at 5 and 10 wt% were obtained from DSC thermograms during heating from room temperature (Process I) or cooling from the melt (Process II). Here, T_{cc}(S), T_{cc}(P), and T_{cc}(E) were evaluated according to the procedure shown in Fig. 8, as reported previously [19,20]. That is, T_{cc}(P) is the peak top temperature of crystallization peak, T_{cc}(S) and T_{cc}(E) are the intersection temperatures of the base line and the tangent lines for the curves in the temperature ranges lower and higher than T_{cc}(P), respectively. The obtained T_{cc}(P) values are plotted in Fig. 9 and the T_{cc}(S), T_{cc}(P), and T_{cc}(E) values are summarized in Table 2.

On heating at a rate of 10 °C min^{-1} (Process I), the T_{cc}(P) of pure PLLA film (108 °C) is in agreement with 106–119 °C reported by Migliaresi et al. for pure PLLA specimens with viscosity-average molecular weights (M_v) of 3.1×10^4–4.3×10^5 g mol^{-1} (heating rate = 5 °C min^{-1}) [28] and with 109 °C reported by ourselves for pure PLLA films ($M_w = 2.2 \times 10^5$ g mol^{-1}) prepared with benzene and dichloromethane (heating rate = 10 °C min^{-1}) [19]. On heating, the addition of C_{60}, SWCNT, and CNH significantly lowered the T_{cc}(P) values (acted as a nucleating agent and accelerated overall crystallization), whereas the addition of CB3855 and CB5500 slightly elevated the T_{cc}(P) values (disturbed the formation of nuclei and delayed overall crystallization). In the cases of CNB and KB, the effects of addition depend on the filler concentration, i.e., at a filler concentration of 5 wt%,

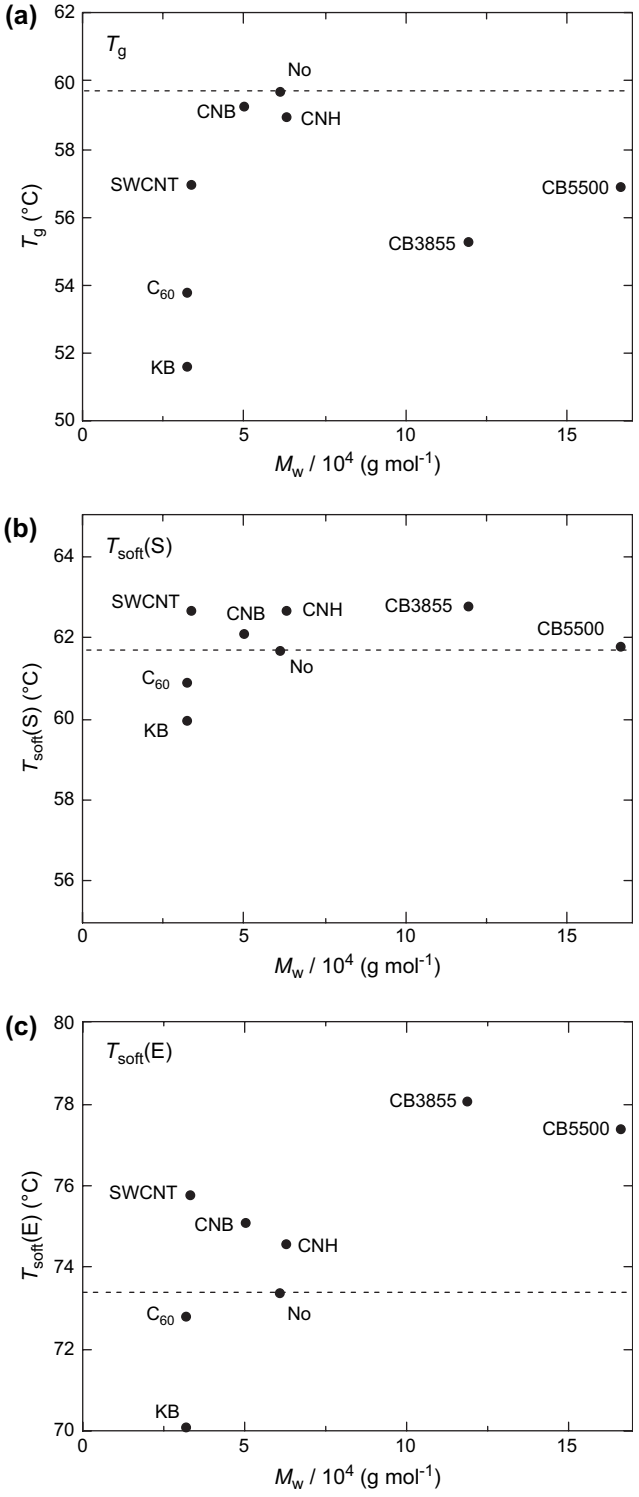

Fig. 7. Glass transition temperature (T_g) (a), starting softening temperature [T_{soft}(S)] (b), and ending softening temperature [T_{soft}(E)] (c) of PLLA films with different carbon fillers (10 wt%) as a function of M_w. Horizontal broken lines in figures show the values for pure PLLA film.

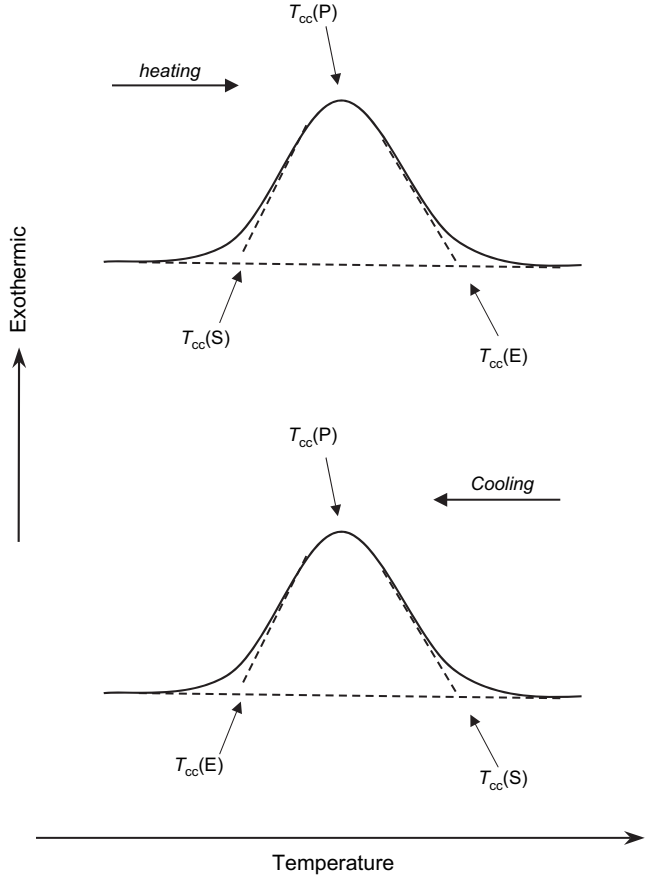

Fig. 8. Procedures for estimating the starting, peak, and ending temperatures of cold crystallization [T_{cc}(S), T_{cc}(P), and T_{cc}(E), respectively].

the T_{cc} values were elevated, but lowered at a filler concentration of 10 wt%.

On cooling at a rate of -3 °C min^{-1} (Process II), the T_{cc}(P) of pure PLLA film (103 °C) is consistent with 106–126 °C reported by Migliaresi et al. (cooling rate = -1 °C min^{-1}) [28] and with 107 and 111 °C reported by ourselves (casting solvents: benzene and dichloromethane, respectively, cooling rate = -1 °C min^{-1}) [19]. The slightly lower T_{cc}(P) value of pure PLLA film in the present study is attributable to a higher cooling rate. The T_{cc}(P) values of PLLA films with carbon fillers, excluding those of KB, were higher than the T_{cc}(P) value of pure PLLA film. This reveals that most of the carbon fillers can act as a nucleating agent for PLLA crystallization during cooling process.

In order to clarify the effects of molecular weight of PLLA on T_{cc} values, the T_{cc}(P) of PLLA films with 10 wt% of fillers is plotted in Fig. 10 as a function of M_w of PLLA. On heating (Process I), the T_{cc}(P) of PLLA increased from 85 to 115 °C with increasing M_w from 3×10^4 to 1.7×10^5 g mol^{-1}. This trend was observed in our previous study for PLLA with different molecular weights [28] and reveals that the T_{cc}(P) is determined by the molecular mobility but not by filler nucleating effects. As suggested earlier the melt-quenching process is expected to induce the formation of self-nuclei [19,29–31], reducing the effects of fillers on T_{cc}(P). In contrast, on cooling (Process II), the T_{cc}(P) was higher for the PLLA films with fillers than for pure PLLA film, except for PLLA–KB(10) film. This reflects that the carbon fillers, excluding KB, effectively act as a nucleating agent.

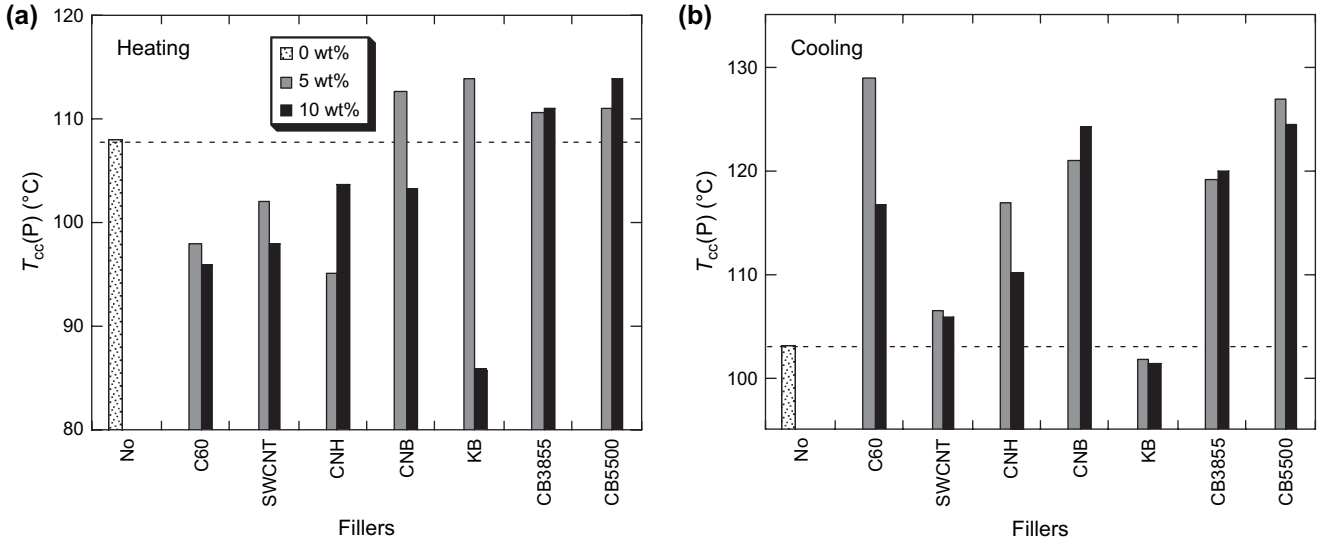

Fig. 9. Peak temperature of cold crystallization [T_{cc}(P)] of PLLA films with different carbon fillers (5 and 10 wt%) on heating from room temperature (Process I) (a) and on cooling from the melt (Process II) (b). Horizontal broken lines show the values for pure PLLA film.

Table 2 shows the obtained non-normalized and normalized ($-\Delta H_{cc}$) values on heating (Process I) and cooling (Process II). On heating at a rate of 10 °C min^{-1} (Process I), the ($-\Delta H_{cc}$) value of pure PLLA film (63 J g^{-1}) was higher than 29–38 J g^{-1} for pure PLLA reported by Migliaresi et al. (5 °C min^{-1}) [28] and 33 and 37 J g^{-1} reported by ourselves (casting solvents: benzene and dichloromethane, respectively, heating rate = 10 °C min^{-1}) [19]. On cooling at a rate of −3 °C min^{-1} (Process II), the ($-\Delta H_{cc}$) value of pure PLLA film (58.0 J g^{-1}) was higher than 32–48 J g^{-1} for pure PLLA [28] reported by Migliaresi et al. (−1 °C min^{-1}) and 36 and 38 J g^{-1} reported by ourselves (casting solvents: benzene and dichloromethane, respectively, heating rate = −1 °C min^{-1}) [19]. The higher ($-\Delta H_{cc}$) values of pure PLLA film on both heating and cooling in the present study should be ascribed to a low molecular weight of PLLA, which was caused by thermal degradation during melt-blending and molding. As seen from Table 2, the normalized ($-\Delta H_{cc}$) values of the PLLA films with carbon fillers were much lower than those of pure PLLA film, on both heating and cooling, irrespective of M_w of PLLA. These findings suggest that the crystalline thickness or size of PLLA decreased, or the amount of non-crystallizable PLLA chains increased upon

Table 2
Cold crystallization of pure PLLA film and PLLA films with different fillers during heating from room temperature (Process I) and cooling from the melt (Process II)

Filler	Content (wt%)	Heating (Process I)					Cooling (Process II)				
		T_{cc}(S)[a] (°C)	T_{cc}(P)[a] (°C)	T_{cc}(E)[a] (°C)	*Non-normalized* ($-\Delta H_{cc}$)[b] (J g^{-1})	*Normalized* ($-\Delta H_{cc}$)[b] (J g^{-1})	T_{cc}(S)[a] (°C)	T_{cc}(P)[a] (°C)	T_{cc}(E)[a] (°C)	*Non-normalized* ($-\Delta H_{cc}$)[b] (J g^{-1})	*Normalized* ($-\Delta H_{cc}$)[b] (J g^{-1})
No	0	97.4	107.9	115.7	62.7	62.7	112.8	102.8	96.7	58.0	58.0
C_{60}	5	90.4	97.9	105.8	34.3	36.1	134.4	128.8	124.8	47.5	50.0
	10	89.8	96.0	101.9	32.9	36.6	125.3	116.7	107.9	40.2	44.7
SWCNT	5	80.7	102.1	110.9	33.0	34.7	120.4	106.5	101.3	37.2	41.3
	10	90.9	98.0	105.3	32.1	35.7	127.0	105.8	99.9	37.4	41.6
CNH	5	88.1	95.1	101.3	40.0	42.1	124.5	116.9	109.0	45.9	48.3
	10	96.8	103.6	110.0	30.8	34.2	123.6	110.1	100.0	36.6	40.7
CNB	5	99.4	112.5	124.1	29.5	31.1	129.8	121.0	115.0	39.4	41.5
	10	95.0	103.2	111.2	33.5	37.2	128.6	124.2	120.0	44.2	49.1
KB	5	87.7	113.9	128.4	30.4	32.0	112.3	101.8	94.5	27.4	28.8
	10	80.2	85.7	95.7	28.5	31.7	115.8	101.3	97.2	33.3	37.0
CB3855	5	98.1	110.7	119.4	30.2	31.8	126.0	119.1	113.3	35.0	36.8
	10	99.5	111.1	120.5	30.8	34.2	125.9	119.9	114.5	37.6	41.8
CB5500	5	96.6	111.1	120.5	29.1	30.6	134.2	126.9	120.0	38.8	40.8
	10	101.2	113.8	123.8	27.0	30.0	132.8	124.4	115.6	31.6	35.1

[a] T_{cc}(S), T_{cc}(P), and T_{cc}(E) are the starting, peak, and ending temperatures of cold crystallization, respectively.
[b] ΔH_{cc} is cold crystallization enthalpy.

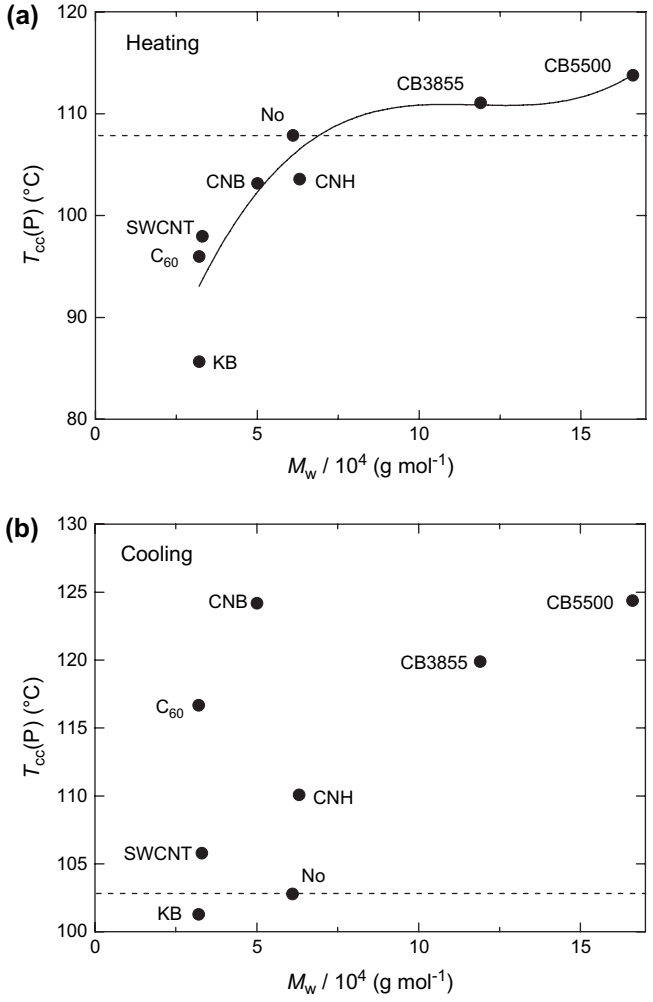

Fig. 10. Peak temperature of cold crystallization [T_{cc}(P)] of PLLA films with different carbon fillers (10 wt%) on heating from room temperature (Process I) (a) and on cooling from the melt (Process II) (b) as a function of M_w. Horizontal broken lines show the values for pure PLLA film.

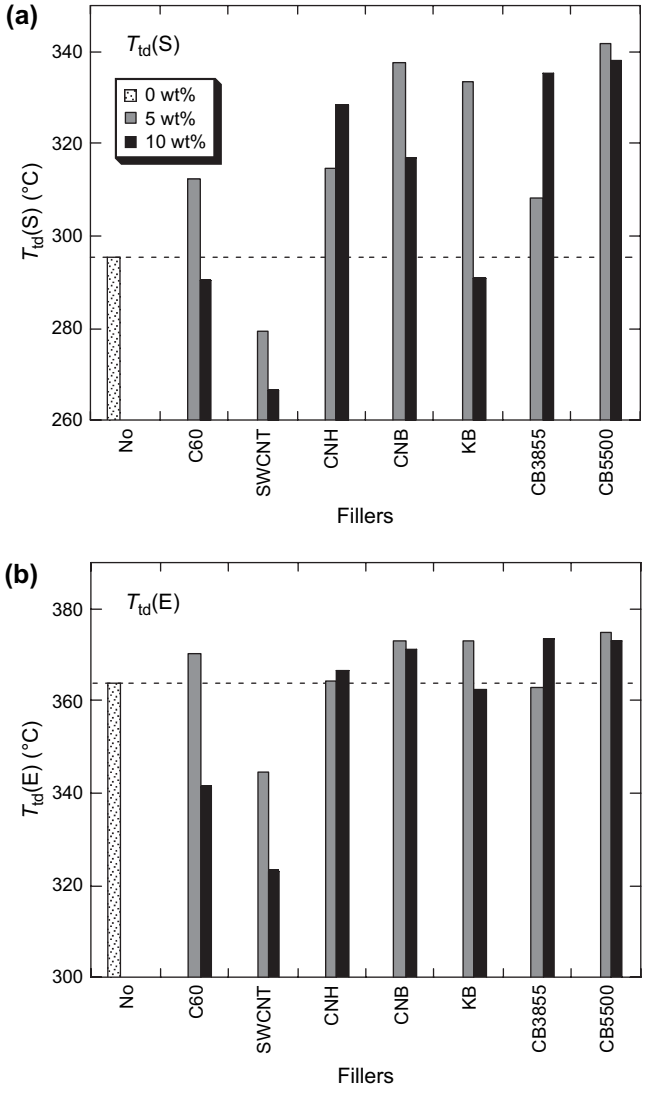

Fig. 11. Starting and ending temperatures of thermal degradation [T_{td}(S) (a) and T_{td}(E) (b), respectively] of PLLA films with different carbon fillers (5 and 10 wt%). Horizontal broken lines show the values for pure PLLA film.

addition of the fillers, although the nucleus number of crystallites increased.

3.4. Thermal degradation

The starting and ending temperatures of thermal degradation [T_{td}(S) and T_{td}(E)] were obtained from the TG curves of PLLA films with different carbon fillers, and are shown in Fig. 11. T_{td}(S) and T_{td}(E) values were estimated using the same procedures for estimating T_{soft}(S) and T_{soft}(E), which are shown in Fig. 6. This procedures are reported in Ref. [32]. The T_{td}(S) and T_{td}(E) values of 295 and 364 °C for pure PLLA are comparable with the reported ones [33–35]. There were three trends for the effects of fillers. The first trend was an increase in thermal degradation temperature with an increase in filler concentration, as in the T_{td}(S) of PLLA–CNH and PLLA–CB3855 films. Probably, in these cases the fillers should have blocked the evaporation of volatile components such as lactides formed by thermal degradation. The second trend was a decrease in thermal degradation temperature with an increase in filler concentration, as in the T_{td}(S) and T_{td}(E) of PLLA–SWCNT film. It is probable that the large aspect ratio of SWCNT (i.e., needle-like structure) disturbed the diffusion of PLLA into the space of loosely assembled SWCNT, the remaining vacant space should have penetrated the film like ‘‘chimney’’, and volatile components formed by thermal degradation could have readily been removed via ‘‘chimney’’, resulting in a rapid increase in weight loss. In other words, the surface area per unit mass was increased by the addition of SWCNT. The third trend was an increase in thermal degradation temperature at 5 wt% and lower thermal degradation temperature at 10 wt% compared with that at 5 wt%. This trend was observed for most of the PLLA films with fillers. The reason for higher degradation temperatures at 5 wt% should be the same as that for PLLA–CNH and PLLA–CB3855 films. On the other hand, the lower degradation temperature at 10 wt% should be the mixed effects of ‘‘barrier’’ and ‘‘chimney’’. If the chimney effect prevails the

barrier effect, the degradation temperature should be lowered, and vice versa. In the present study, CB5500 was the most effective filler at both concentrations for enhancement of thermal stability. The effects of M_w of PLLA on thermal degradation temperature are shown in Fig. 12. It seems that T_{td}(S) increased with increasing M_w, whereas T_{td}(E) was independent of M_w for M_w exceeding 5×10^4 g mol^{-1}. Although the difference in M_w affects the thermal degradation temperature values, the addition of CNH, CNB, CB3855, and CB5500 effectively enhanced the thermal degradation-resistance of PLLA films.

3.5. Enzymatic degradation

As reported earlier, the proteinase K-catalyzed degradation rate is determined by the type, concentration, shape, dimension, dispersion, and adhesion of fillers [36,37]. For further analysis for determining the dispersion and adhesion of fillers, we have carried out proteinase K-catalyzed enzymatic degradation of PLLA films with 10 wt% of fillers. Fig. 13 shows

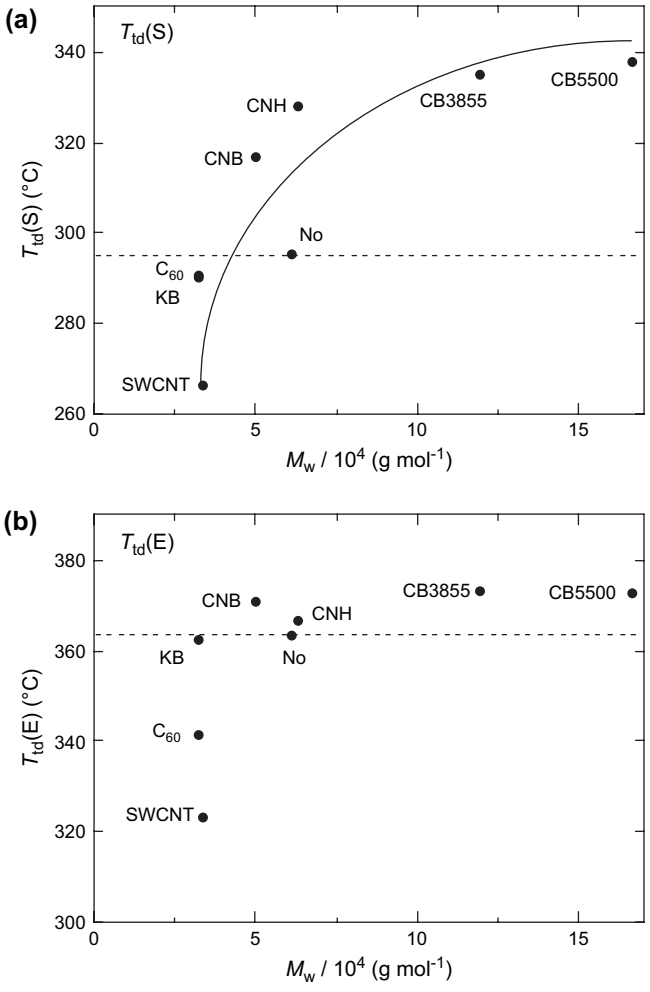

Fig. 12. Starting and ending temperatures of thermal degradation [T_{td}(S) (a) and T_{td}(E) (b), respectively] of PLLA films with different carbon fillers (10 wt%) as a function of M_w. Horizontal broken lines show the values for pure PLLA film.

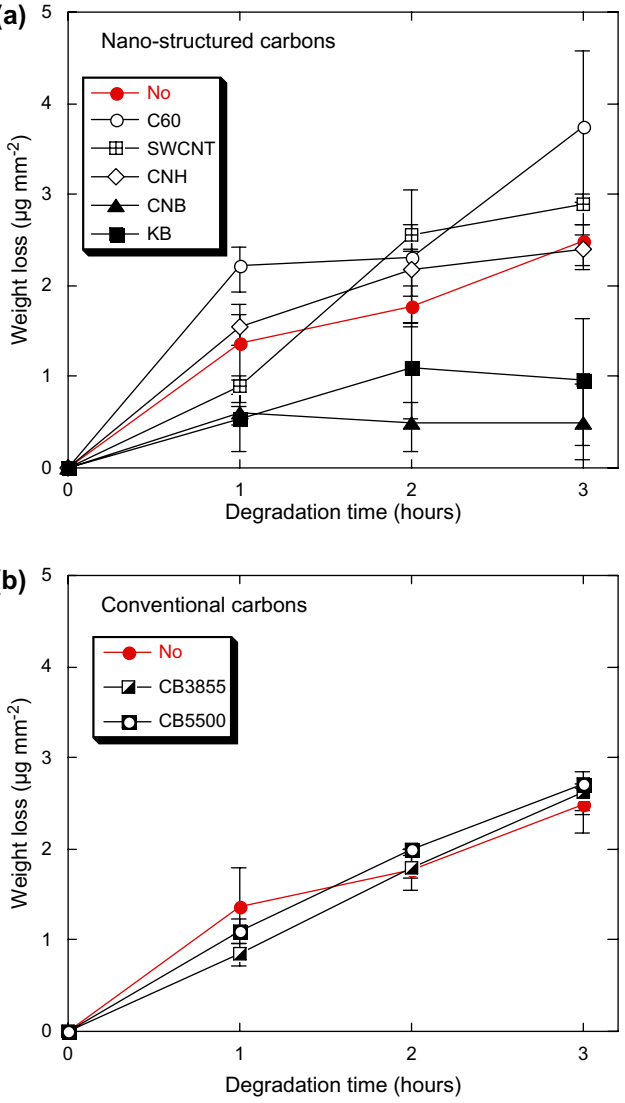

Fig. 13. Weight loss of PLLA films with different nano-structured (a) and conventional carbon (b) fillers (10 wt%) with respect to enzymatic degradation.

the weight loss of PLLA films with respect to proteinase K-catalyzed enzymatic degradation. As seen, C_{60} and SWCNT accelerated the enzymatic degradation. It is expected from low T_{td}(S) and T_{td}(E) values of PLLA−C_{60}(10) and PLLA−SWCNT(10) films (i.e., from chimney effect of C_{60} and SWCNT) that there should have been relatively large gap between PLLA phase and C_{60} or SWCNT assemblies for proteinase K to diffuse into. As a result, the enzymatic degradation could occur inside the film as well as on the film surface. Moreover, as expected from the lack of adhesiveness of C_{60} or SWCNT to PLLA phase, it seems that the C_{60} or SWCNT assemblies should have been readily released from the film surface, forming porous structure. The formation of porous structure is known to accelerate the enzymatic degradation of a biodegradable polyester [38]. The two factors, the effects of "gap" and "facile release", should have increased the enzymatic degradation rate. In contrast, the addition of KB

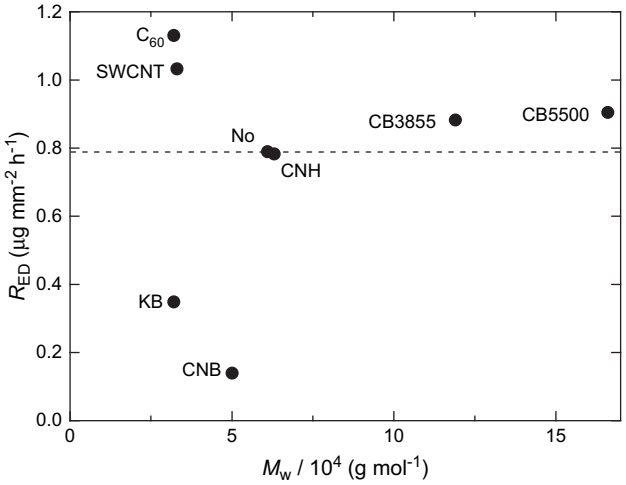

Fig. 14. Weight loss rate (R_{ED}) of PLLA films with different carbon fillers (10 wt%) as a function of M_w. Horizontal broken lines show the value for pure PLLA film.

and CNB diminished the enzymatic degradation rate. Probably, the particles of KB and CNB were well dispersed in the films and the ones on the film surface should have disturbed the direct access of proteinase K to PLLA chains, resulting in low initial degradation rate and saturation of weight loss at a long degradation time. In this case, the adhesiveness of fillers to PLLA phase should have been high to block proteinase K to diffuse into the film. For most of the carbon fillers, the accelerating effects by ''gap between PLLA phase and carbon fillers'' and ''facile release of carbon fillers'' should have been balanced with the disturbing effect by ''blocking'', and therefore, the experimental weight loss of PLLA films with fillers was similar to that of pure PLLA film. From comparison between Fig. 13(a) and (b), it can be concluded that conventional carbons have very small effects on the enzymatic degradation rate, whereas the effects of nano-structured carbons largely varied depending on the size, shape, and dimension. The average enzymatic degradation rate (R_{ED}) values were estimated from the slopes of weight loss lines, and are plotted in Fig. 14 as a function of M_w. It is reported that R_{ED} increased with decreasing molecular weight [39]. However, no such trend was observed for the PLLA films with carbon fillers. Therefore, the R_{ED} is confirmed to depend on the shape, dimension, dispersion, and adhesion of carbon fillers and their assembled structures.

Figs. 15 and 16, respectively, show the SEM images of the PLLA films with different carbon fillers after enzymatic degradation for 3 h, and the SEM image of the pure PLLA film before enzymatic degradation. In Fig. 16, only the image for pure PLLA film is shown, because the surface morphology of PLLA films with different carbon fillers was very similar to that of pure PLLA film. The surface before enzymatic degradation had many parallel grooves, which should have reflected the surface morphology of polyimide sheets used for compression of PLLA films. As seen in Fig. 14, all film surfaces became rougher after enzymatic degradation and the roughness was highest for the PLLA–C_{60} film. In other words, the film surface after enzymatic degradation was determined by the weight loss values rather than by the shape, dimension, dispersion, and adhesion of carbon fillers. However, in the case of PLLA–SWCNT film, despite the second largest weight loss after 3 h of enzymatic degradation, it showed a small surface change.

4. Conclusions

From the aforementioned experimental results the following conclusions can be derived for the effects of fillers on the conductivity, thermal properties, crystallization, and enzymatic degradation of PLLA.

(1) The addition of carbon fillers decreased the ρ values of PLLA films. Among the carbon fillers, SWCNT was the most effective filler to reduce the ρ of PLLA film. The addition of SWCNT lowered the ρ of PLLA film from $1.6 \times 10^5\ \Omega\,cm$ (filler concentration = 0 wt%) to the values lower than $1 \times 10^2\ \Omega\,cm$ (filler concentration of 10 wt%). The crystallization of PLLA further decreased the ρ values. Furthermore, even the addition of 1 wt% SWCNT caused dramatic decrease in ρ from 1.6×10^5 to $3–4 \times 10^3\ \Omega\,cm$. Such high effects of SWCNT can be ascribed to its needle-like structure, which obliges SWCNT to effectively contact with each other.

(2) The addition of carbon fillers, except for C_{60} and CNB at 5 wt%, lowered the glass transition temperature, whereas the addition of carbon fillers, excluding C_{60}, elevated softening temperatures, if an appropriate filler concentration was selected. This indicates that the addition of carbon fillers, except for C_{60}, was effective to enhance the dimensional stability of PLLA films on heating. It seems that the molecular (particle) size of C_{60} was too small to support the external force on heating.

(3) On heating from room temperature, the T_{cc}(P) was determined, mainly by the molecular weight of PLLA, whereas on cooling from the melt, the carbon fillers, excluding KB, elevated the T_{cc}(P), indicating the effectiveness of most of the carbon fillers as nucleating agents. Despite the nucleating effects, the addition of the carbon fillers decreased the normalized ($-\Delta H_{cc}$) of PLLA on both heating and cooling.

(4) The addition of CNH, CNB, CB3855, and CB5500 was effective for the enhancement of thermal stability of PLLA films, whereas the addition of SWCNT reduced the thermal stability. The addition of other fillers increased the thermal stability of PLLA at 5 wt%, whereas the thermal stability at 10 wt% was lower than that at 5 wt%. In such a case thermal degradation rate should have been determined by the balance between an enhancement effect of ''blocking'' and a reducing effect of ''chimney''.

(5) The addition of C_{60} and SWCNT significantly enhanced the enzymatic degradation, whereas the addition of KB and CNB disturbed the enzymatic degradation. It seems that the enzymatic degradation rate of the PLLA films

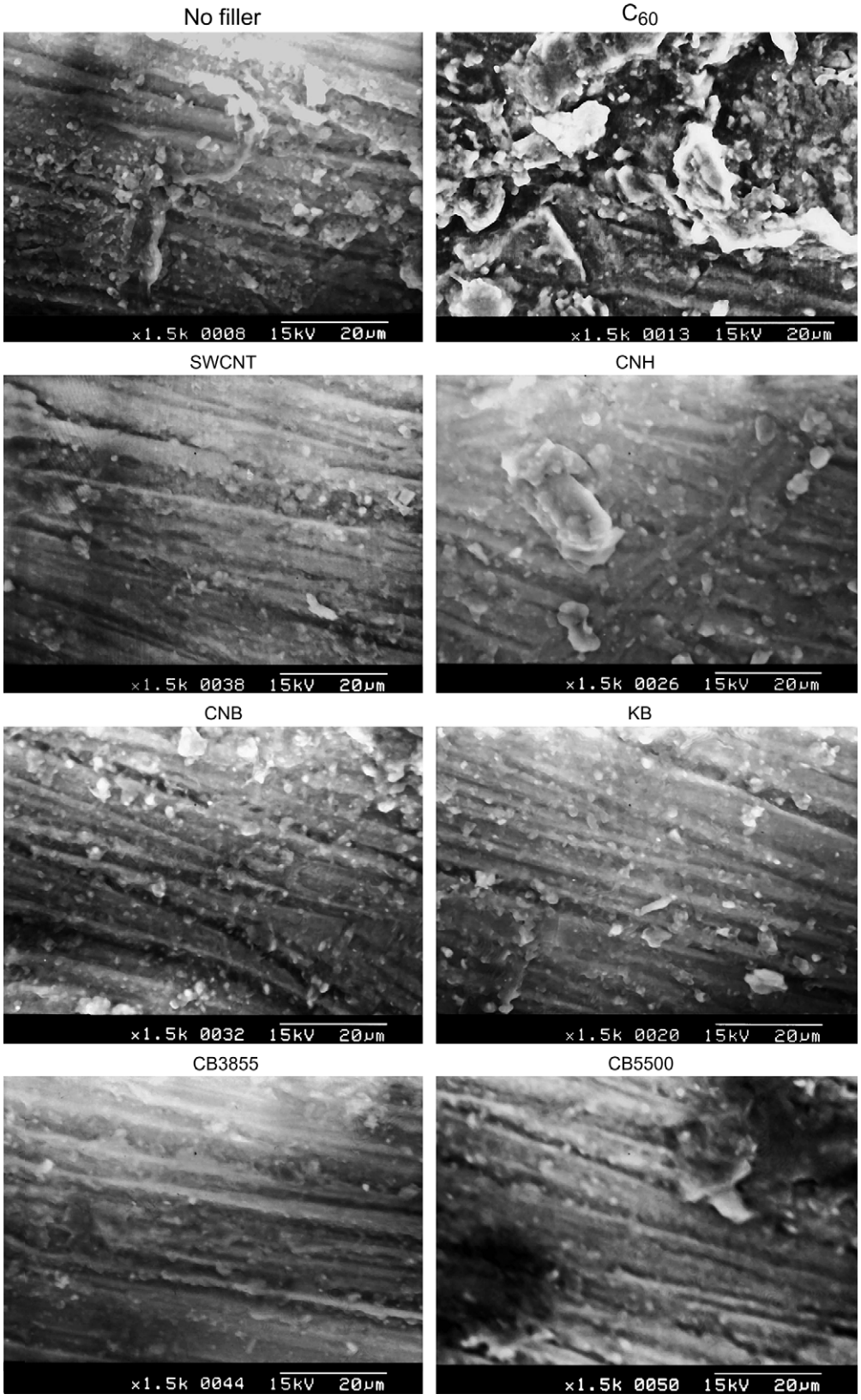

Fig. 15. SEM images of PLLA films with different carbon fillers (10 wt%) after enzymatic degradation for 3 h.

with fillers was determined by the diffusibility of proteinase K between PLLA phase and fillers and by the releasability of fillers from PLLA phase during enzymatic degradation, both of which should have enhanced the enzymatic degradation, and by the blocking effect by fillers, which should have disturbed the enzymatic degradation.

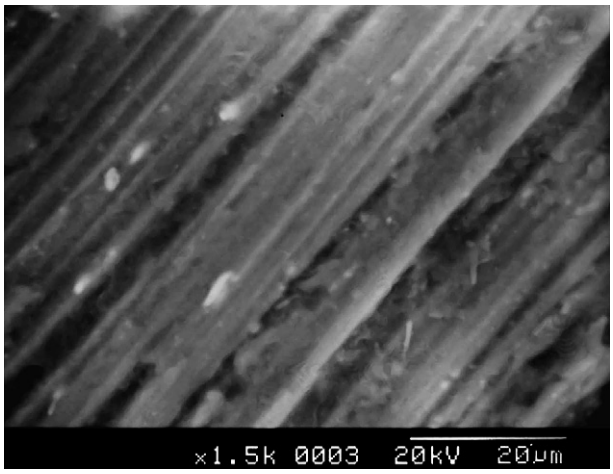

Fig. 16. SEM images of pure PLLA film before enzymatic degradation.

Acknowledgements

We are grateful to Professor Dr. Shinichi Itsuno, from the Department of Materials Science, Toyohashi University of Technology, for the use of polarimeter, to Mr. Kazunobu Yamada, from the Research and Development Center, Unitika Ltd., for giving us PLLA used in the present study, and to Mr. Junichi Narita, from Development and Research Center, Tohcello Co. Ltd., for supplying us polyimide sheets used for the molding of PLLA films. This research was supported by a Grant-in-Aid for Scientific Research on Priority Area, ''Sustainable Biodegradable Plastics'' No. 11217209 and The 21st Century COE Program, ''Ecological Engineering for Homeostatic Human Activities'', from the Ministry of Education, Culture, Sports, Science and Technology (Japan) and a Grand-in-aid for Scientific Research, Category ''C'', No. 16500291, from Japan Society for the Promotion of Science (JSPS).

References

[1] Kharas GB, Sanchez-Riera F, Severson DK. In: Mobley DP, editor. Plastics from microbes. New York: Hanser Publishers; 1994. p. 93–137.
[2] Doi Y, Fukuda K, editors. Biodegradable plastics and polymers. Amsterdam (The Netherlands): Elsevier; 1994.
[3] Coombes AGA, Meikle MC. Clin Mater 1994;17:35–67.
[4] Vert M, Schwarch G, Coudane JJ. Macromol Sci Pure Appl Chem 1995;A32:787–96.
[5] Hartmann MH. In: Kaplan DL, editor. Biopolymers from renewable resources. Berlin (Germany): Springer; 1998. p. 367–411.
[6] Ikada Y, Tsuji H. Macromol Rapid Commun 2000;21:117–32.
[7] Garlotta D. J Polym Environ 2001;9:63–84.
[8] Albertsson A-C, editor. Degradable aliphatic polyesters. Advances in polymer science, vol. 157. Berlin (Germany): Springer; 2002.
[9] Södergård A, Stolt M. Prog Polym Sci 2002;27:1123–63.
[10] Scott G, editor. Biodegradable polymers: principles and applications. 2nd ed. Dordrecht, The Netherlands: Kluwer Academic Publishers; 1995.
[11] Tsuji H. In: Doi Y, Steinbüchel A, editors. Polyesters 3. Biopolymers, vol. 4. Weinheim, Germany: Wiley-VCH; 2002. p. 129–77.
[12] Auras R, Harte B, Selke S. Macromol Biosci 2004;4:835–64.
[13] Thakur KAM, Kean RT, Zupfer JM, Buehler NU, Doscotch MA, Munson EJ. Macromolecules 1996;29:8844–51.
[14] Schmidt SC, Hillmyer MA. J Polym Sci Part B Polym Phys 2001; 39:300–13.
[15] Urayama H, Kanamori T, Fukushima K, Kimura Y. Polymer 2003; 44:5635–41.
[16] Ke T, Sun X. J Appl Polym Sci 2003;89:1203–10.
[17] Wang C, Guo Z-X, Fu S, Wu W, Zhu D. Prog Polym Sci 2004;29:1079–141.
[18] Sinha Ray S, Okamoto M. Prog Polym Sci 2003;28:1539–641.
[19] Tsuji H, Takai H, Fukuda N, Takikawa H. Macromol Mater Eng 2006; 291:325–35.
[20] Tsuji H, Takai H, Saha SK. Polymer 2006;47:3826–37.
[21] Xu G, Niwa H, Imaizumi T, Takikawa H, Sakakibara T, Yoshikawa K, et al. New Diamond Front Carbon Technol 2005;15:73–81.
[22] Niwa H, Higashi K, Shinohara K, Takikawa H, Sakakibara T, Yoshikawa K, et al. Smart Process Technol 2006;1:57–60.
[23] Reeve MS, McCarthy SP, Downey MJ, Gross RA. Macromolecules 1994;27:825–31.
[24] Bueche F. J Appl Phys 1973;44:532–3.
[25] Sumita M, Sakata K, Asai S, Miyasaka K, Nakagawa H. Polym Bull 1991;25:265–71.
[26] Lee J-C, Nakajima K, Ikehara T, Nishi T. J Appl Polym Sci 1996; 65:409–16.
[27] Chen Q, Bin Y, Matsuo M. Macromolecules 2006;39:6528–36.
[28] Migliaresi C, De Lollis A, Fambri L, Cohn D. Clin Mater 1991;8: 111–8.
[29] Tsuji H, Miyase T, Tezuka Y, Saha SK. Biomacromolecules 2005;6: 244–54.
[30] Tsuji H, Ikada Y. Polymer 1995;36:2709–16.
[31] Tsuji H, Ikada Y. Polymer 1996;37:595–602.
[32] Cam D, Marucci M. Polymer 1997;38:1879–84.
[33] Aoyagi T, Yamashita K, Doi Y. Polym Degrad Stab 2002;76:53–9.
[34] Tsuji H, Fukui I. Polymer 2003;44:2891–6.
[35] Fan Y, Nishida H, Shirai Y, Tokiwa Y, Endo T. Polym Degrad Stab 2004;86:197–208.
[36] Fukuda N, Tsuji H, Ohnishi Y. Polym Degrad Stab 2002;78:119–27.
[37] Fukuda N, Tsuji H. J Appl Polym Sci 2005;96:190–9.
[38] Tsuji H, Ishizaka T. J Appl Polym Sci 2001;80:2281–91.
[39] Tsuji H, Miyauchi S. Biomacromolecules 2001;2:597–604.